Journal of Electronic Materials, Vol. 22, No. 8, 1993

Band Gap Uniformity and Layer Stability of HgTe-CdTe Superlattices Grown by Photon-Assisted Molecular Beam Epitaxy

R.W. YANKA, K.A. HARRIS, L.M. MOHNKERN, A.R. REISINGER, and T.H. MYERS*

Electronics Laboratory, General Electric Co. (now Martin Marietta Corp.),
Syracuse, NY 13221

N. OTSUKA

School of Materials Engineering, Purdue University, West Lafayette, IN
47907

Two material properties important to the application of HgTe/CdTe superlattices for device fabrication are band gap uniformity and thermal stability. In this paper, we present the results of an infrared photoluminescence study of (211)B HgTe/CdTe superlattices grown by photon-assisted molecular beam epitaxy which show that cut-off wavelength uniformity can be controlled to a level commensurate with the demands of advanced infrared detector fabrication. Infrared photoluminescence and transmission electron microscopy were also employed to demonstrate that (211)B HgTe/CdTe superlattices are less prone to interdiffusion than previously believed.

Key words: HgTe/CdTe superlatice, interdiffusion in superlattices, PAMBE, TEM

INTRODUCTION

HgTe/CdTe superlattices (SLs) were first proposed more than a decade ago as an alternative to HgCdTe alloy structures for the fabrication of long-wave infrared (LWIR) detectors.[1] Early theoretical work indicated that at a given cut-off wavelength HgTe/CdTe superlattices could offer several advantages over the equivalent alloy, particularly in the very long-wave infrared (VLWIR) regime.[2] The first theoretical band structure calculations for (211)B oriented HgTe/CdTe superlattices were reported in 1990 by Hoffman et al.[3] It has only been recently, however, that superlattices with material properties appropriate for device applications have been demonstrated. In particular, the application of photon-assisted molecular beam epitaxy (PAMBE) to the growth of HgTe/CdTe superlattices has resulted in epilayers with excess carrier lifetimes of several hundred nanoseconds[4] as well as the first demonstration of high quantum efficiency superlattice photodiodes.[5]

One important material property required for the practical fabrication of LWIR and VLWIR superlattice detector arrays is that the band gap must not vary significantly across the area of the wafer. This property is essential to insure uniform response. This paper reports the results of infrared photoluminescence (IRPL) mapping measurements made on HgTe/CdTe superlattice epilayers grown by photon-assisted molecular beam epitaxy. Measurements were made at various positions across the SL layer, from which the variation of the band gap across the sample was determined. Our measurements indicate that SL band gaps for material grown in our laboratory (without rotation), exhibit uniformities suitable for array fabrication over areas as large as 2 cm². This result is important because it demonstrates that the PAMBE technique is capable of producing uniform Hg-based

---

(Received October 12, 1992; revised January 13, 1993)

*Present address: Department of Physics, West Virginia University, Morgantown, WV 26506, USA

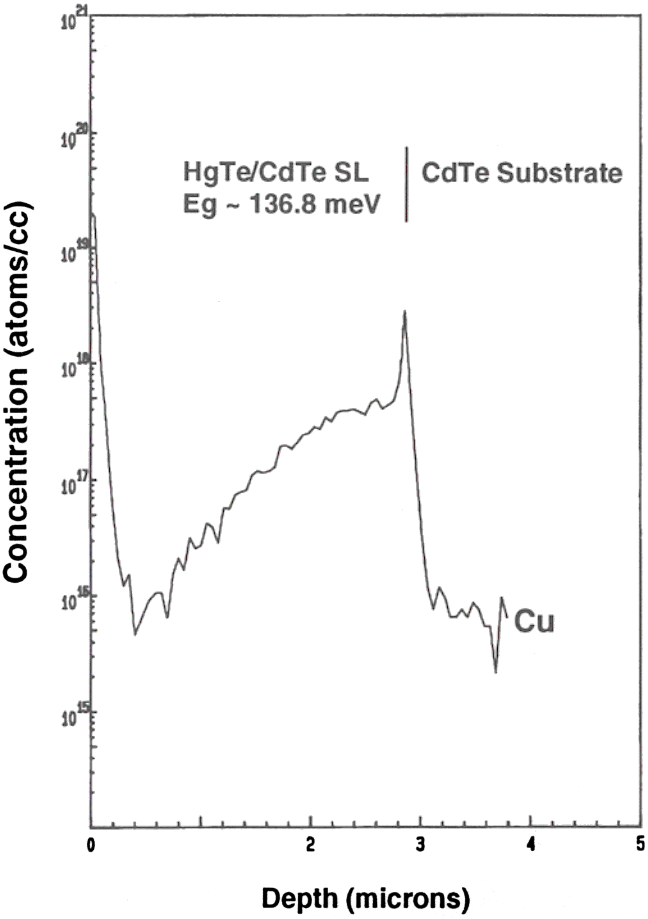

Fig. 1. Secondary ion mass spectroscopy copper profile of an As-doped superlattice grown on a copper contaminated CdTe substrate. Copper levels in the substrate and in the near surface region of the epilayer are at the SIMS detection limit.

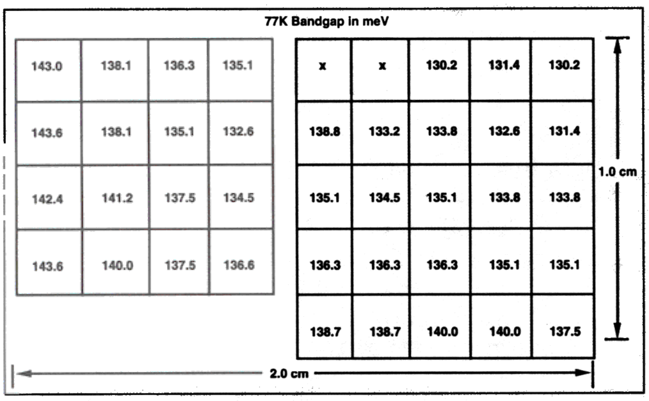

143.0	138.1	136.3	135.1
143.6	138.1	135.1	132.6
142.4	141.2	137.5	134.5
143.6	140.0	137.5	136.6

x	x	130.2	131.4	130.2
138.8	133.2	133.8	132.6	131.4
135.1	134.5	135.1	133.8	133.8
136.3	136.3	136.3	135.1	135.1
138.7	138.7	140.0	140.0	137.5

Fig. 2. Infrared photoluminescence band gap map of an LWIR superlattice. The average energy gap is 136.8 meV with σ = 3.5 meV, which is equivalent to a cut-off wavelength of 9.09 μm with σ = 0.23 μm. The measured uniformity is over a 2 × 1 cm area and is in a range acceptable for the fabrication of detector arrays.

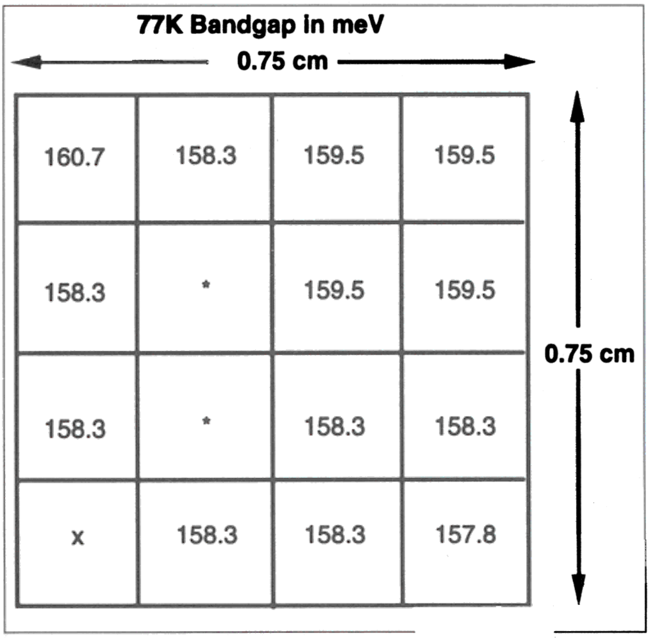

160.7	158.3	159.5	159.5
158.3	*	159.5	159.5
158.3	*	158.3	158.3
x	158.3	158.3	157.8

Fig. 3. Infrared photoluminescence band gap map of an superlattice exhibiting an average energy gap of 158.8 meV with σ = 0.8 meV. The equivalent λ_c is 7.81 μm with σ = 0.04 μm as measured over the 0.5 cm^2 area of the sample.

epilayers suitable for IR applications.

Infrared photoluminescence mapping was also used to evaluate the thermal stability of HgTe/CdTe superlattices. This is an important issue since there have been reports of significant interdiffusion of the HgTe and CdTe constituent layers of (111)B oriented superlattices at temperatures as low as 110°C.[6,7] For this study, IRPL measurements were carried out at 77K to determine the SL band gap at various points across the free surface of an epilayer. The sample was then flipped over and corresponding IRPL measurements were made through the transparent substrate. Any variations observed due to layer interdiffusion would be manifested by band gap variations between the corresponding measurements. Preliminary results suggest that SL layer interdiffusion does not occur, to the limit of the measurement, during PAMBE growth. These measurements have also produced evidence of 2-D carrier confinement at the superlattice/substrate interface.

EXPERIMENTAL DETAILS

HgTe/CdTe superlattice epilayer growth was performed in one of two custom MBE machines modified for PAMBE growth. These systems have been described in an earlier publication.[5] All of the epilayers were grown on (211)B CdTe substrates at a deposition temperature of 170°C.[8] The substrates were prepared using standard wet-etch techniques followed by thermal processing prior to growth.[8,9] Typical beam equivalent pressures used for the source ovens were 3–5 × 10^{-4} Torr for Hg, 1–3 × 10^{-6} Torr for Te, and 5–10 × 10^{-7} Torr for CdTe. Overall growth rates employed were in the range of 0.5 to 1.0 μm/h. The Te and Cd sources were shuttered alternately to produce the superlattice structure. The Hg source was not shuttered, resulting in a constant Hg overpressure throughout the growth. This produced barrier layers consisting of $Hg_{1-x}Cd_xTe$, where x = 0.85–0.90.

It has recently been reported that the presence of copper in commercially available substrate materials can have a profound effect on the properties of HgCdTe epilayers grown on these substrates.[10] We have found that this problem extends to HgTe/CdTe superlattices as well, even though they are not exposed to high temperature anneals after growth. Figure 1 shows a secondary ion mass spectroscopy (SIMS) copper profile obtained from an arsenic-doped superlattice grown on a copper contaminated substrate. This superlattice exhibited a band gap of 136.8 meV. A copper diffusion profile is observed emanating from the substrate-epilayer interface and dropping down to SIMS background levels about 1 μm from the film surface. In order to overcome this problem, we have developed a technique for removing copper from commercially available (211)B substrates. This treatment allows the growth and processing of device quality alloy and superlattice epilayers with no apparent copper contamination as measured by SIMS.[11] All epilayer growth at Martin Marietta is currently being carried out on substrates subjected to our copper extraction technique.

Infrared photoluminescence[12] measurements were carried out using a 500 mW CW Nd:YAG laser as the excitation source. The pump beam was focused on a sample mounted in a Janis liquid-helium cryostat equipped with a ZnSe window. A resistive heating element in the cryostat and its associated control circuitry permitted regulation of sample temperature between 10 and 400K. Measurements for this study were carried out at a sample temperature of 77K. The IRPL photon flux was collected and collimated by a set of ZnSe lenses and directed to the input port of a Nicolet 60SX Fourier transform infrared spectrometer (FTIR) equipped with a liquid-nitrogen cooled MCT photovoltaic detector with a nominal cut-off wavelength of 13 μm. Both the cryostat and the input port of the (FTIR) feature ZnSe windows. A Ge filter

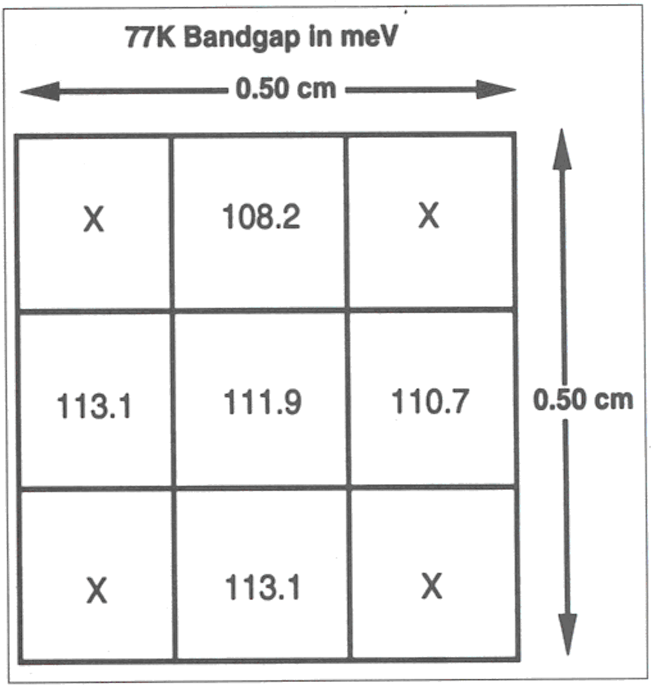

X	108.2	X
113.1	111.9	110.7
X	113.1	X

Fig. 4. Infrared photoluminescence cut-off map of a LWIR superlattice. The average band gap of this sample is 111.4 meV with σ = 2.0 meV, which is equivalent to λ_c = 11.13 μm with σ = 0.21 μm. This uniformity is equivalent to the corresponding alloy with x = 0.218 and σ = 0.0013.

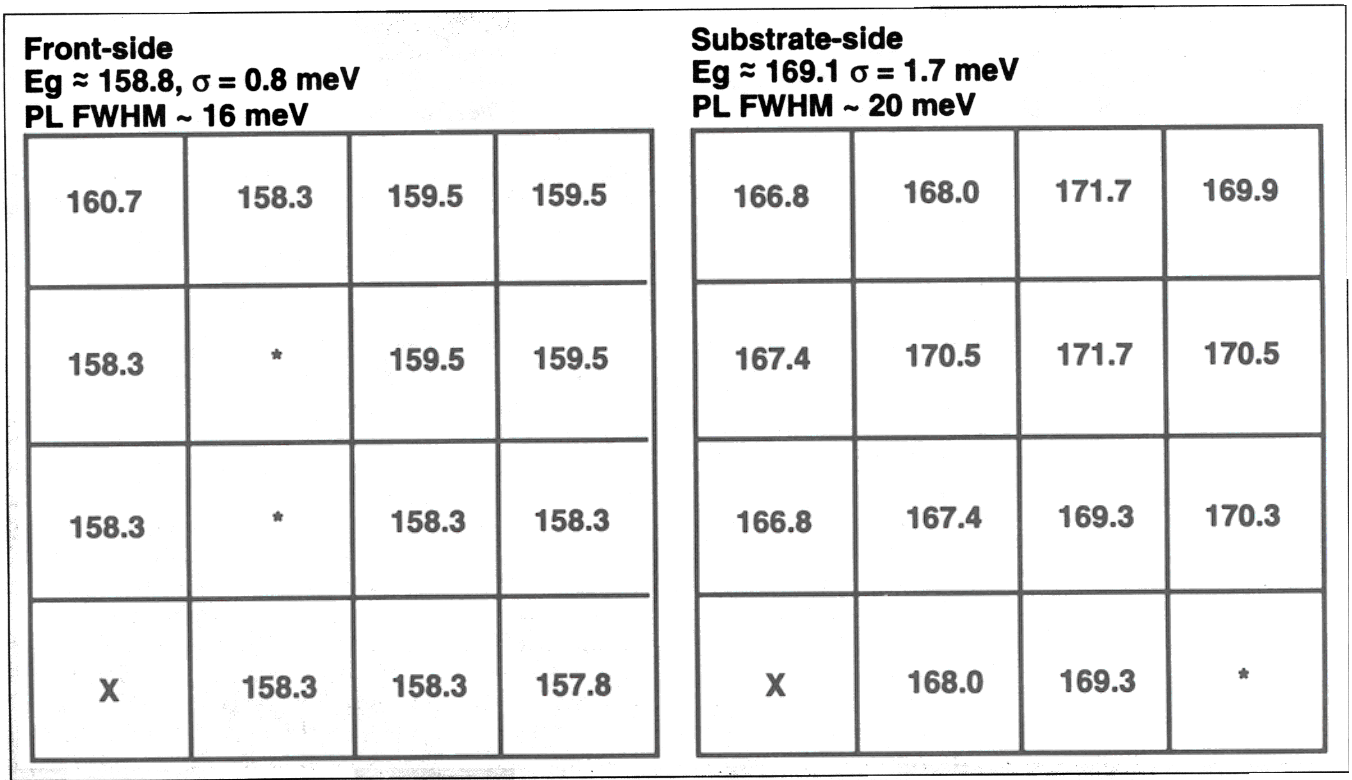

Front-side
Eg ≈ 158.8, σ = 0.8 meV
PL FWHM ~ 16 meV

160.7	158.3	159.5	159.5
158.3	*	159.5	159.5
158.3	*	158.3	158.3
X	158.3	158.3	157.8

Substrate-side
Eg ≈ 169.1 σ = 1.7 meV
PL FWHM ~ 20 meV

166.8	168.0	171.7	169.9
167.4	170.5	171.7	170.5
166.8	167.4	169.3	170.3
X	168.0	169.3	*

Fig. 5. Comparison map of frontside vs backside IRPL band gaps. The band gaps agree to within 10 meV, indicating minimal interdiffusion is taking place during film growth. Measurements were made at 77K.

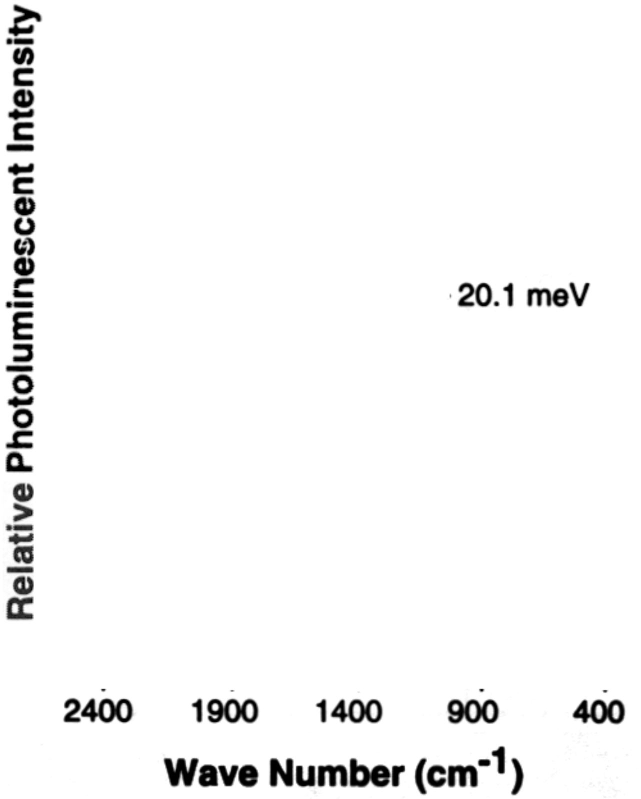

Fig. 6. Representative 77K IRPL peak obtained from the backside of the sample depicted in Fig. 5. The multiple peaks superimposed on the high energy side of the IRPL peak are the signature of quantized transitions.

located before the spectrometer's input port was used to filter out the 1.06 μm pump radiation.

RESULTS AND DISCUSSION

Infrared photoluminescence provides a direct measurement of the band gap of a superlattice in the near surface region. Since the spot size used is relatively small (~ 400 μm diameter in this case), it is possible to probe several areas and produce a band gap energy map for the sample under study. Such a map is shown in Fig. 2 for a 2 × 1 cm SL epilayer. The average energy gap for this sample is 136.8 meV with a standard deviation of $\sigma = 3.5$ meV. This is equivalent to a cutoff wavelength of 9.07 μm with $\sigma = 0.23$ μm, which is suitable for detector array fabrication. A high degree of band gap uniformity can also be seen in the data depicted in Fig. 3 for a 0.75 × 0.75 cm sample. This superlattice exhibits an average energy gap of 158.8 meV with $\sigma = 0.83$ meV, which corresponds to a cutoff of $\lambda_c \sim 7.8$ μm with a σ of 0.04 μm. Finally, Fig. 4 shows a cut-off map for an LWIR superlattice with $\lambda_c \sim 11.13$ μm with $\sigma = 0.21$ μm. A comparison of this sample with an alloy of comparable band gap shows that the PAMBE grown superlattice exhibits an equivalent alloy x-value variation of $\sigma = 0.0013$.

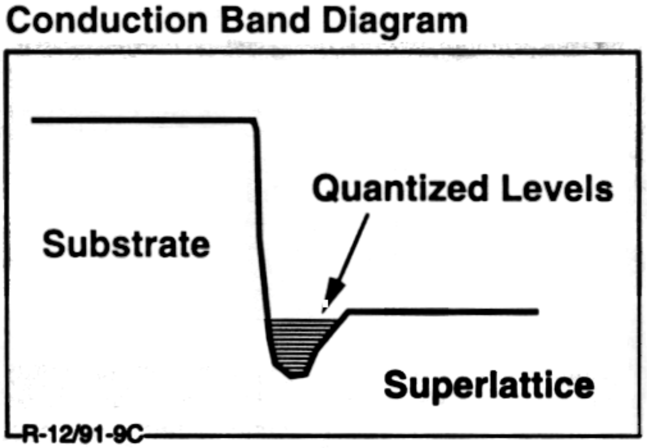

Fig. 7. Schematic representation of the quantum well at the substrate-epilayer interface. Carriers in this quantum well are two-dimensional with quantized energy levels. This model could explain the multiple transitions observed in the IRPL spectrum in Fig. 6.

It is important to note that substrate rotation during epilayer deposition is not utilized in the MBE system in which the superlattices for this study were grown. Furthermore, these growths employed only one Te source situated 12° off the center growth line. We are currently studying the use of a second Te source placed so as to compensate for the interactions experienced with the high flux from the Hg source. This modification should significantly increase the yield of epilayers exhibiting a high degree of band gap uniformity.

Interdiffusion between superlattice constituent layers was investigated by comparing IRPL band gap maps obtained from the film surface with those obtained at the epilayer/substrate interface (IRPL excitation through the substrate). Figure 5 shows such a comparison obtained from a superlattice grown at Martin Marietta. The band gap variations are within 10 meV, suggesting that minimal interdiffusion takes place during PAMBE growth. This is the first directly measured evidence that the temperatures associated with the PAMBE growth process do not seriously affect the integrity of the superlattice layers.

Figure 6 shows a typical IRPL peak measured at the epilayer/substrate interface of the superlattice depicted in Fig. 5. All of the "backside" spectra exhibited several peaks superimposed on the higher energy side of the main peak. This result may be indicative of 2-D carriers confined at the interface between the substrate and epilayer. Such carriers have been observed in IR magneto-absorption measurements made on this and other superlattices grown at Martin Marietta.[13] Other groups have also reported 2-D carriers in the substrate/epilayer interface region of (211)B HgTe/CdTe superlattices.[3] Two-dimensional carriers confined at the substrate/epilayer interface would exhibit quantized energy levels as shown in Fig. 7. These energy levels could give rise to the additional peaks observed in the IRPL spectrum and tend to broaden and skew the main IRPL peak. This mechanism may be responsible for the 10 meV variation between the front-side and substrate-side IRPL measurements.

To further investigate the integrity of the superlattice layers in the near substrate region, TEM microscopy was performed at Purdue University on the sample depicted in Fig. 5. The constituent layers in the vicinity of the substrate were subjected to a temperature of 170°C for a period of several hours (the growth time of the film). The micrograph in Fig. 8 shows the interface between the superlattice and the (211)B substrate on which it was deposited. The HgTe (dark) and CdTe (light) layers are sharp and well defined all the way down to the substrate with no evidence of interdiffusion. This provides strong evidence that the 10 meV band gap difference seen in Fig. 5 is not due to layer interdiffusion during film growth.

Post-growth anneals have also been used to investigate the thermal stability of HgTe/CdTe superlattices grown at Martin Marietta. Selected epilayers have been subjected to temperatures between 100 and 180°C. Pre- and post-anneal energy gap measurements were then used to determine whether superlattice layer interdiffusion had occurred. Preliminary results indicate that post-growth anneals at temperatures as high as 180°C have little effect on the cut-off wavelength of the HgTe/CdTe superlattices studied. For example, a sample subjected to 180°C for 75 min showed no apparent change in band gap. These initial results suggest that HgTe/CdTe superlattices are more robust than first thought, and bodes well for the development of processes for the fabrication of device structures from this material system.

SUMMARY

Infrared photoluminescence analysis was used to show that (211)B HgTe/CdTe superlattices can be grown by PAMBE which exhibit uniformities in cut-off wavelength suitable for IR detector array fabrication. We have also demonstrated that these materials are more thermally stable than previously thought in the community. Epilayer growth temperatures of 170°C and exposure to post-growth anneals of up to 180°C were found to have little effect on the cut-off wavelengths of the samples studied. These results represent an important step toward the development of an IR detector array technology based on HgTe/CdTe superlattice materials.

ACKNOWLEDGMENT

Work supported by the Air Force Wright Laboratory Materials Directorate under contract No. F33615-90-C-5922, contract monitor Ms. L.E. Brown.

REFERENCES

1. J.B. Schulman and T.C. McGill, *Appl. Phys. Lett.* 34, 663 (1979).
2. D.L. Smith, T.C. McGill and J.N. Schulman, *Appl. Phys. Lett.* 43, 180 (1983).
3. C.A. Hoffman, J.R. Meyer, R.J. Wagner, F.J. Bartoli, X. Chu, J.P. Faurie, L.R. Ram-Mohan and H. Xie, *J. Vac. Sci. Technol.* A 8, 1200 (1990).
4. A.R. Reisinger, K.A. Harris, T.H. Myers, R.W. Yanka and L.M. Mohnkern, *Appl. Phys. Lett.* 61, 699 (1992).
5. K.A. Harris, T.H. Myers, R.W. Yanka, L.M. Mohnkern and N. Otsuka, *J. Vac. Sci. Technol.* B9, 1752 (1991).
6. D. Arch, J.P. Faurie, J.-L. Staudenmann, M. Hibbs-Brenner

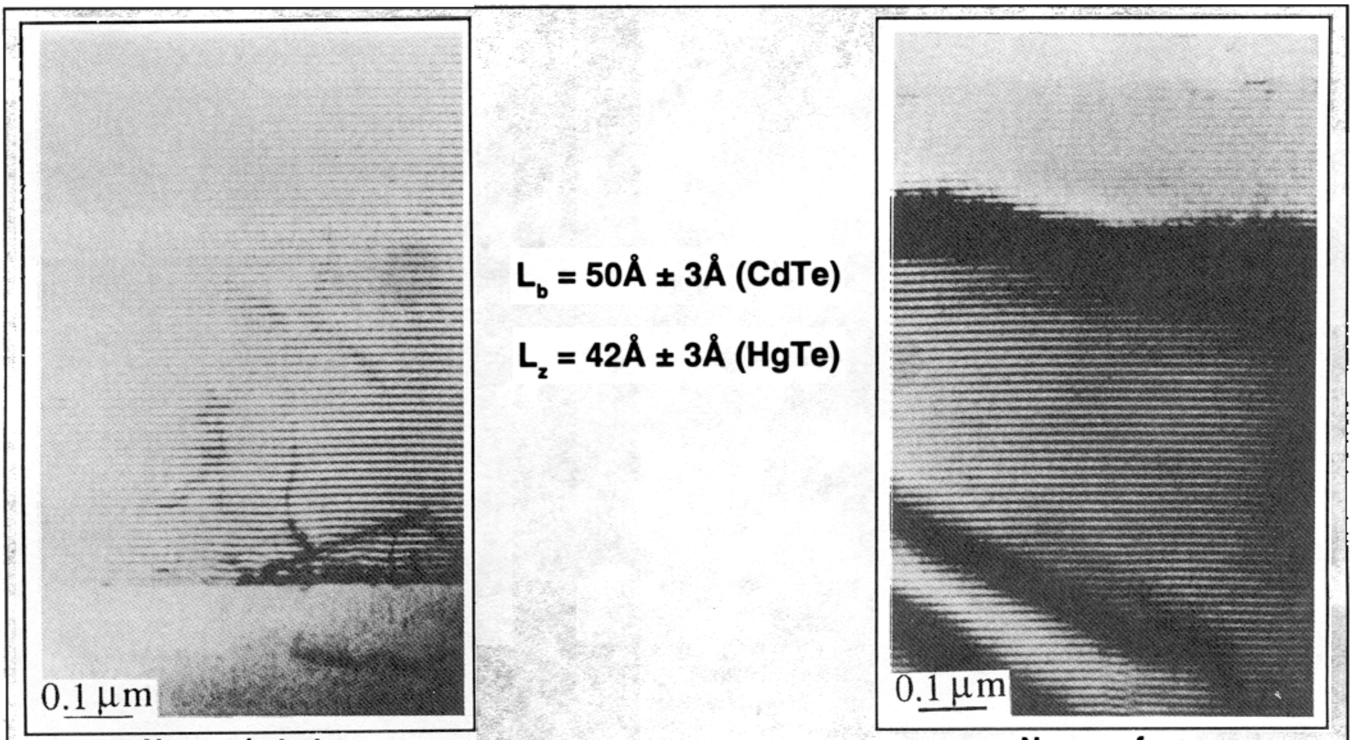

Near-substrate **Near-surface**

Fig. 8. Cross-sectional TEM micrograph of the substrate-epilayer interface and near-surface region of the superlattice depicted in Fig. 5. The constituent layers are sharply defined all the way down to the substrate. This demonstrates that interdiffusion of superlattice layers during film deposition does not occur to the limit of this measurement technique.

and P. Chow, *J. Vac. Sci. Technol.* A 4, 2101 (1986).
7. D. Arch, J.-L. Staudenmann and J.P. Faurie, *Appl. Phys. Lett.* 48, 1588 (1986).
8. K.A. Harris, S. Hwang, D.K. Blanks, J.W. Cook, Jr., J.F. Schetzina and N. Otsuka, *J. Vac. Sci. Technol.* A 4, 2061 (1986).
9. T.H. Myers, R.W. Yanka, J.P. Karins, K.A. Harris, J.W. Cook, Jr. and J.F. Schetzina, *Mater. Res. Soc. Symp. Proc.* 90, 295 (1987).
10. T.H. Myers, K.A. Harris, R.W. Yanka, L.M. Mohnkern, R.J. Williams and G.K. Dudoff, *J. Vac. Sci. Technol.* B 10, 1438 (1992).
11. K.A. Harris, R.W. Yanka, L.M. Mohnkern, R.J. Williams, G.K. Dudoff and T.H. Myers, submitted to *Appl. Phys. Lett.*
12. A.R. Reisinger, R.N. Roberts, S.R. Chinn and T.H. Myers, *Rev. Sci. Instrum.* 60, 82 (1989).
13. K.A. Harris, R.W. Yanka, L.M. Mohnkern, A.R. Reisinger, T.H. Myers, Z. Yang, Z. Yu, S. Hwang and J.F. Schetzina, *J. Vac. Sci. Technol.* B 10, 1574 (1992).